THE EFFECT OF THE BIAS MAGNETIC FIELD ON THE MAGNETOSTRICTIVE SENSOR PERFORMANCE IN FLEXURAL WAVE-BASED DAMAGE DETECTION IN A CYLINDER

Woochul Kim[1] and Yoon Young Kim
[1]Seoul National University, Seoul, South Korea

Abstract: Flexural wave measurements for non-destructive evaluation in waveguides have received much attention recently. The main motivation to use dispersive flexural waves is that longitudinal waves employed for non-destructive evaluation often go through mode conversion into flexural waves as in curved regions. The objective of this investigation is to investigate the effect of the static bias magnetic field on the measured output of a magnetostrictive non-contact sensor for flexural waves. Unlike measuring longitudinal waves by the magnetostrictive sensor, the sensor output for flexural wave measurement is affected significantly by the applied bias magnetic field distribution. In this work, we will consider a few bias magnetic configurations to reject the longitudinal waves but capture only the flexural waves, and investigate their performance through several flexural wave experiments. Specially, we will consider the measurements of flexural waves in cracked solid cylinders in which the flexural waves are generated by ball drops perpendicular to the cylinders. Through these experiments, it will be addressed that small cracks are difficult to diagnose without using an optimal bias magnetic system. The signals measured by the magnetostrictive sensors were analyzed in the time-frequency plane for accurate damage assessment.

Introduction: When time-varying mechanical loads are applied to a ferromagnetic material, the magnetic field distribution within the material changes. This phenomenon is known as the inverse magnetostriction effect or the Villari effect[1-2]. The magnetostrictive or magnetomechanical sensor measures elastic strain waves in ferromagnetic materials based on this phenomenon. Other sensors, based on electromechanical or piezoelectric principles may also be used to measure elastic waves, but only the magnetostrictive sensor has the non-contact measurement capability. In addition, the magnetostrictive sensor has a simple configuration: the sensor simply consists of coils surrounding the specimen and one or more bias permanent magnets. The change in the magnetic flux density within the ferromagnetic material is converted to the voltage change in the surrounding coil.

Thus far, applications of magnetostrictive sensors have mostly focused on the measurement of longitudinal and torsional waves in ferromagnetic waveguides. Recently, however, the sensor has also been used for the measurement of flexural vibrations and waves[3]. A recent paper[4] shows that when the sensor is employed for flexural wave measurement, the location of the bias magnets must be carefully selected. Cho *et al*[5]. proposed an optimal shape of the permanent magnet and Kim and Kim[6-7] also proposed the bias magnetic system using optimized yoke shape obtained by topology optimization for high-performance magnetostrictive sensors applicable for the measurement of flexural waves propagating in ferromagnetic waveguides. The magnetostrictive sensor using yokes instead of permanent magnet have merits in that it can be adjusted the strength of the bias magnetic field and cost-effective in comparison with permanent magnet. Our objective in the present research is to investigate the effect of the bias magnetic field generated by these optimized yokes on the measured signal output. Especially, we focus on flexural wave-based damage detection in a solid cylinder.

The ball drop method has been used as a standard method to generate elastic flexural waves[8-9]. The ridge analysis procedure is employed to estimate instantaneous frequencies by the continuous Gabor wavelet transform (GWT)[9] that is utilized as an effective and powerful time-frequency analysis tool for identifying rapidly-varying dispersive wave signals.

Analysis: *A. Bias Magnetic System Design Optimization*

In this work, we will consider the measurement of flexural waves in a long solid ferromagnetic cylindrical waveguide shown in Fig. 1. The voltage output of the coil shown in Fig. 1 results from the magnetic field change of the ferromagnetic cylinder at $x=x_s$ by the elastic flexural wave. One can show[3] that the voltage output $V(x_s,t)$ can be written as

$$V(x_s,t) = Enc_1 \frac{\partial^2 \theta(x_s,t)}{\partial t \partial x} \int_A B^b(x_s,y) y dA \tag{1}$$

where B^b is the magnetic flux density along the x axis. In Eq. (1), c_1 is a constant and n is the number of turns of a

coil. Young's modulus and the rotation of the cylinder cross section are denoted by E and θ, respectively. From Eq. (1), we immediately see that the maximum sensor output $V(x,t)$ for flexural wave measurement will be obtained when the integral is maximized. Therefore, if we maximize the following integral $f(x_s)$, the performance of the sensor will be maximized:

$$f(x_s) = \int_A B_x^b(x_s, y) y dA \tag{2}$$

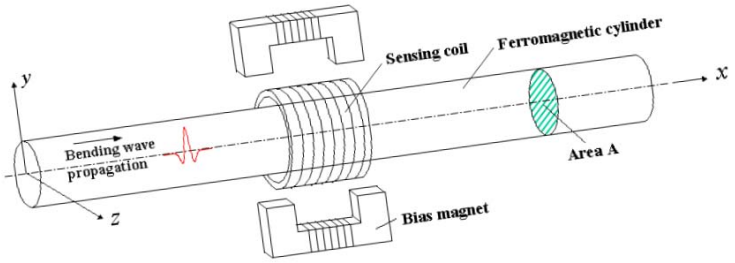

Fig.1. The application of the magnetostrictive sensor consisting of a coil and bias magnets for flexural wave measurement in a long ferromagnetic cylinder.

In order to maximize the voltage output $V(x,t)$ of the sensor coil, the following maximization problem can be set up:

$$\text{Maximize} : f = \sum_{i=1}^{n_y^s} B_x^b(x_s = L, y_i; \rho_e) \times y_i \ , \ \text{Subject to} : h(\rho_e) = \sum_{e=1}^{n_d} \rho_e v_e - M_0 \le 0 \tag{3}$$

Kim and Kim[6-7] used the topology optimization method[6-7] to find the optimal yoke shape. Equation (3) is the discretized version of Eq. (2) by the finite element method of a design region for the bias yoke, where n^s_y denotes the number of nodes in the y direction in the solid cylinder at $x=x_s$, and n_d is the total number of the density design variables ρ_e. These variables are assigned to all finite elements in the design domain. The inequality in Eq. (3) is the statement of the constraint imposed on the total mass M_0 of the bias yoke, where v_e is the element area.

The optimized yoke configurations[7] by the topology optimization method are given in Fig. 2.

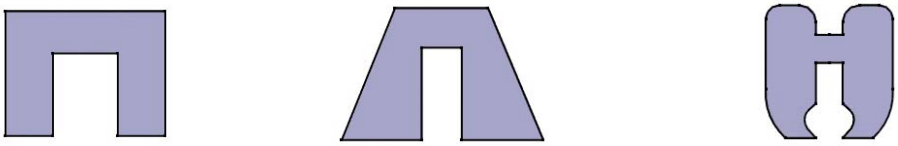

(a) (b) (c)

Fig. 2. Three different yokes of the magnetostrictive sensor. (a) The baseline yoke (b) the optimized yoke by the linear topology optimization (c) the optimized yoke by the nonlinear topology optimization.

B. Continuous wavelet transform (*CWT*)

CWT is a time- frequency analysis tool which is very effective in analyzing local features of a signal. For a sqaure-integrable signal $f(t)$, the continuous wavelet transform Wf is defined as[10],

$$Wf(u,s) = \int_{-\infty}^{+\infty} f(t)\psi_{u,s}^*(t)dt = \int_{-\infty}^{+\infty} f(t)\frac{1}{\sqrt{s}}\psi^*(\frac{t-u}{s})dt \tag{4}$$

where $(\bullet)^*$ denotes the complex conjugate of $(\bullet)$. The function $\psi(t)$ in Eq. (4) is a mother wavelet satisfying the following condition

$$\int_{-\infty}^{+\infty} \frac{|\hat{\psi}(\omega)|^2}{|\omega|} d\omega < \infty \tag{5}$$

where $\hat{\psi}(\omega)$ is the Fourier transform of $\psi(t)$. The weak condition for existence of integral in Eq. (5) is

$$\hat{\psi}(\omega) = 0, \quad i.e. \quad \int_{-\infty}^{+\infty} \psi(t) dt = 0 \tag{6}$$

The function $\psi_{u,s}(t)$ is obtained by scaling $\psi(t)$ by the scaling parameter s and translating it by the translation parameter u.

In the present research, the Gabor wavelet is employed as the mother wavelet $\psi(t)$:

$$\psi(t) = g(t) e^{i\eta t} \tag{7}$$

$$g(t) = \frac{1}{(\sigma^2 \pi)^{1/4}} e^{-t/2\sigma^2} \tag{8}$$

where η is the center frequency of $\hat{\psi}(\omega)$ and σ represents the time spread of $\psi(t)$. The Gabor wavelet is controlled by the product G_s of η and σ,

$$G_s = \eta \sigma \tag{9}$$

By adjusting the value G_s, the Gabor wavelet of a desirable shape can be obtained.

C. Experiments

We conducted several experiments to investigate the effect of the yoke configuration on the magnitude of the measured signal.

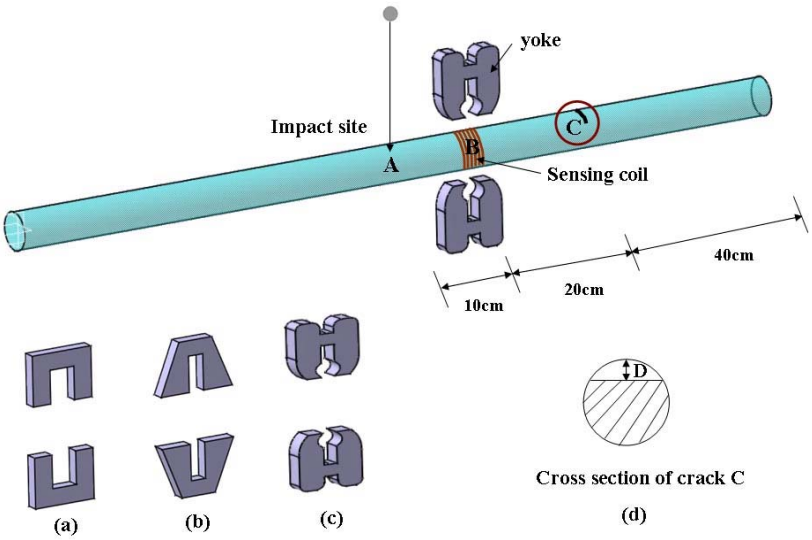

Fig. 3. Experimental setup for a solid circular beam excited by a steel ball at the center.

In Fig.3, a cracked beam is simply supported. The beam is excited by a steel ball dropped at the center of the beam marked by A. Flexural waves generated by the impact were measured by a magnetostrictive sensor with different yoke configurations at the sampling rate of 20 μsec at point B.

The beam has a small crack at location C and Fig. 3(d) shows the shape and size of the crack. For the time-frequency analysis of the measured signals by the sensor, the continuous Gabor wavelet with G_s=3.5 was used as the mother wavelet.

The data used to configure the experimental system are as follows:

- Cylindrical test rod:

material = mild steel, length = 1.4 m, diameter = 10 mm, crack size =2 mm and 3mm

- Projectile: material = mild steel, diameter = 10 mm, length = 30 mm, mass = 17.4 g

(The head is machined to be hemi-spherical in order to ensure point impact.)

- Sensing coils: position = 0.6 m from the right end, made of 100 turns of 0.12 mm copper wires (Installed over an acryl bobbin).
- Coils in the electromagnet: 50 turns of 0.3 mm copper wires, nominal current density = 3.5 A/mm^2.

The analyzed signals by CWT are shown in Fig. 4 for D=3 mm and Fig. 5 for D=2 mm. The signals were measured at B by employing the three yokes shown in Fig. 3 for the crack size D=3 mm. Figure 4 shows that the flexural waves were successfully captured with the three yoke configurations; the dispersive characteristics of flexural waves are apparent in the time-frequency plane. The time in Fig. 4 and Fig. 5 implies the arrival time of a wave having a certain frequency component. The thick dotted lines in the figures represent the ridges that correspond to the loci of the local maximum points of the scalogram $|Wf(u,s)|$. In Fig. 4, the scale parameter s is converted to the frequency f using the following relation[11],

$$s \cong \frac{f_s \eta}{2\pi f} \tag{10}$$

where f_s is the sampling frequency of the signal $f(t)$. The symbol u in $Wf(u,s)$ stands for the time in Fig. 4 and Fig. 5.

The waves reflected from the crack at C were marked in the middle of the contour plots. For the frequency range between 10 kHz and 30 kHz giving smooth ridges, the signal measured using with the yoke in Fig. 3(c) were the best; The measured signals for D=2 mm were given in Fig. 5

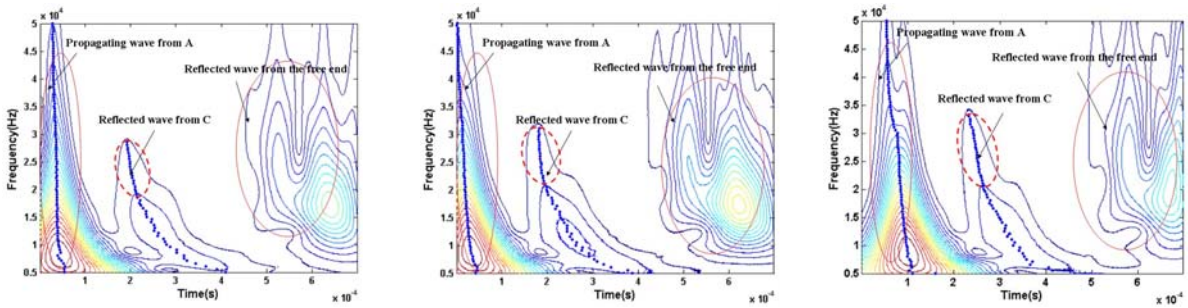

(a) (b) (c)

Fig. 4. The scalogram and the corresponding ridges for the signal measured at B in a beam shown in Fig. 3 with G_s=3.5 and D=3mm by using (a) yoke in Fig. 3(a) (b) yoke in Fig. 3(b) (c) yoke in Fig. 3(c)

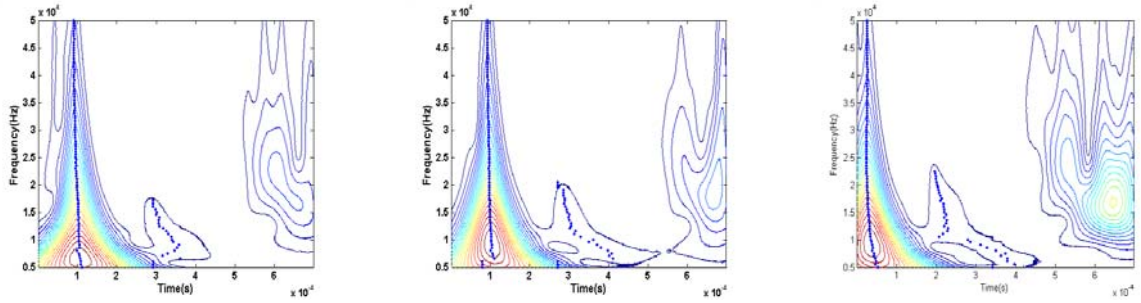

(a) (b) (c)

Fig. 5. The scalogram and the corresponding ridges for the signal measured at B in a beam shown in Fig. 3 with G_s=3.5 and D=2mm (a) yoke in Fig. 3(a) (b) yoke in Fig. 3(b) (c) yoke in Fig. 3(c)

Let us now examine the magnitude of the wave signals along a specific frequency. The magnitude $|Wf|$ is plotted

along f (frequency) = 15 kHz in Fig. 6. In Fig. 6(a), the magnitude of the signal measured by the yoke in Fig. 3(b) is larger by 37% than the corresponding magnitude of the baseline yoke in Fig. 3(a). The additional increase of about 10% is achieved by using the yoke of Fig. 3(c). In Fig. 6(b), the peak magnitudes by the yokes in Fig. 3(b) and Fig. 3(c) for D=2 mm increase by 60% and 73%, respectively, in comparison to the corresponding value of the baseline yoke. This result shows the importance of using optimal bias magnetic systems in accurate signal analysis especially for small cracks. When damage size is quite small, the reflected wave from a crack is hidden within noise, and the bias yoke optimization becomes important. Since the sensor performance is influenced by the magnetic flux density distribution, it is worth examining the distribution at $x=x_s$ (see Fig. 7). The magnetic flux density distributions by ANSYS for the three yokes are plotted in Fig.7. The static magnetic flux density distribution by the yoke in Fig. 3(b) is very close to that by the yoke in Fig. 3(c). This appears due to the fact that the shapes of the yoke tips near the sensing point are similar.

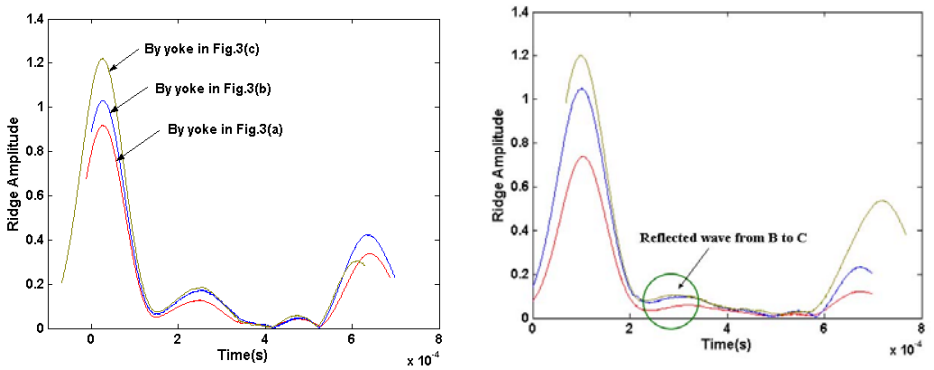

(a) (b)

Fig. 6. Ridge magnitude at 15 kHz (a) D=3 mm (b) D=2 mm

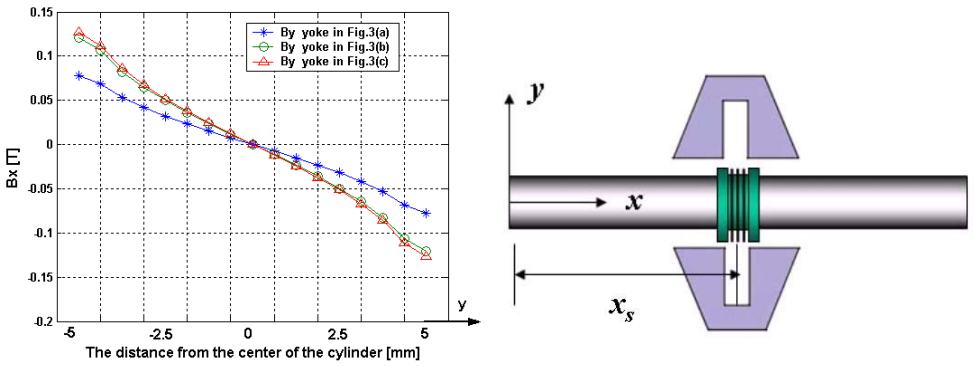

Fig. 7. The magnetic flux density distributions along y by the use of the three yokes shown in Fig. 3(a-c).

Finally, we attempted to estimate the damage location C using the measured signal in Fig. 4 for D=3 mm. In order to estimate the distance d (from B to C), we used

$$d(f) = C_g(f)\frac{\Delta t(f)}{2} \tag{10}$$

where Δt is the difference between the arrival times of the propagating wave from A and the first reflected wave. Note that the group velocity $C_g(f)$ is found from the experimentally measured signal. As can be seen from Fig. 8, the damage location can be estimated most accurately by the using signals obtained by the optimized yokes in Fig. 3(b) and (c).

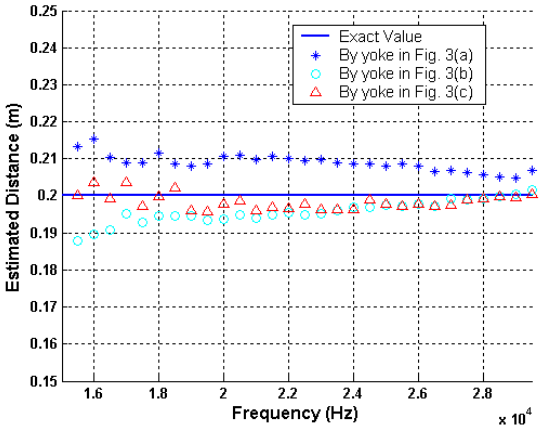

Fig. 8. Estimated distance from the measurement location B to damage location using the ridges of the normalized scalogram (d_{exact}= 0.2 m)

Conclusions: This work was concerned with the investigation of the effect of a bias magnetic system on the performance of a magnetostrictive sensor in measuring elastic flexural waves in a long cylinder. The actual experiments were conducted in cracked long solid cylinders. Two optimized bias yoke configurations were considered and their performance was compared with the performance of the baseline yoke configuration. The performance was checked in terms of the quality of the ridge of the reflected wave from a small crack in the time-frequency plane and in terms of the signal magnitude at a specific frequency. The experiment results showed that the optimized yokes improve the performance of the magnetostrictive sensor. The optimized yoke by the nonlinear topology optimization performed better than the optimized yoke the linear topology optimization although the improvement was not so significant.

References: [1]D. C. Jiles, "Theory of the magnetomechanical effect," *J. Phys. D: Applied Physics*, Vol. 28, pp. 1537-1546, 1995

[2]J. P. Joule, "On the effects of magnetism upon the dimensions of iron and steel bars," *Phy. Mag*. Vol. 3 pp. 30-76, 1847

[3]H. Kwun and C. M. Teller, "Magnetostrictive generation and detection of longitudinal, torsional, and flexural waves in a steel rod," *J. Acoust. Soc. Am*., Vol. 3(2), pp. 1202-1204, 1994

[4]H. Lee and Y. Y. Kim, "Wave selection Using a Magnetomechanical sensor in a solid cylinder," *J. Acoust. Soc. Am.*,Vol. 112(3), pp 953-960, 2002

[5]S. H. Cho, Y. Kim, and Y. Y. Kim, "The Optimal Design and Experimental Verification of the Bias Magnet Configuration of a Magnetostrictive Sensor for Flexural Wave Measurement," *Sensors and Actuators: A Physical,* Vol. 107, pp 225-232, 2003

[6]Y. Y. Kim and W. Kim, "Yoke Topology optimization of the Bias Magnetic System in a Magnetostrictive Sensor," *KSME (Korean Society of the Mechanical Engineers) Journal A (in Korean)*, submitted, 2003

[7]W. Kim and Y. Y. Kim," Design of a Bias Magnetic System of a Magnetostrictive Sensor for Flexural Wave Measurement," *IEEE Trans. Mag*, accepted, 2004

[8]J. F. Dolye, *Wave Propagation in Structures*, Springer-Verlag, New York, 1997

[9]Y. Y. Kim and E.-H. Kim, "Effectiveness of the continuous wavelet transform in the analysis of some dispersive elastic waves," *J.Acoust.Soc.*,Vol. 110(1), pp 86-94, 2001

[10]S. Mallat, *A wavelet tour of signal processing*, Academic press, San Diego, 1998

[11]J.-C. Hong and Y. Y. Kim, "Determination of the Optimal Gabor Wavelet Shape for the Best Time-Frequency Localization Using the Entropy Concept," *Experimental Mechanics*, accepted, 2004